Open access • Posted Content • DOI:10.1101/2021.06.28.450182

Regulation of Myoepithelial Differentiation in 3-Dimensional Culture — Source link

Renee F. Thiemann, Scott Varney, Nicholas Moskwa, John M. Lamar ...+2 more authors

Institutions: Albany Medical College, State University of New York System

Published on: 19 Sep 2021 - bioRxiv (Cold Spring Harbor Laboratory)

Topics: Myoepithelial cell

The Transcriptional Co-Activator Taz Contributes to the Differentiation of a Salivary Gland Epithelial Cell Line Towards a Myoepithelial Phenotype

Renee F.Thiemann[1‡], Scott Varney[2†], Nicholas Moskwa[4], John Lamar[3], Melinda Larsen[3], and Susan E. LaFlamme[1*]

[1]Department of Regenerative and Cancer Cell Biology, [2]Department of Surgery, and [3]Department of Molecular and Cellular Physiology, Albany Medical College, 47 New Scotland Avenue, Albany NY 12208 and [4]Department of Biological Sciences, University at Albany, State University of New York, 1400 Washington Avenue, Albany New 12222.

Running Title: Myoepithelial differentiation

Key words: myoepithelial, TAZ, salivary gland

*Corresponding authors: laflams@amc.edu
‡Current Address: Catholic Central High School, Troy, New York 12182
†Current Address: Department of Cancer Biology, Thomas Jefferson University, Philadelphia, PA 19107

Summary Statement

Identification of a transcriptional co-regulator as a contributor to myoepithelial differentiation in three-dimensional cell culture

Abstract

Myoepithelial cells serve as contractile units in exocrine glands, including mammary, salivary, and lacrimal glands, and their dysfunction negatively impacts secretory function. In spite of their importance, mechanisms that regulate myoepithelial differentiation are poorly defined. To study this process, we employed an established murine salivary gland epithelial cell line, mSG-PAC-1, that we previously demonstrated recapitulates aspects of acinar cell differentiation when cultured as spheroids. Here, we report that mSG-PAC1 spheroids can be induced towards a myoepithelial phenotype by manipulating culture conditions, resulting in the inhibition of expression of the acinar marker, AQP5, the upregulation of myoepithelial markers αSMA, calponin, and the integrin β4 subunit, as well as the acquisition of myoepithelial morphology. Transcriptome analysis indicated that YAP/TAZ target genes are also upregulated. We demonstrate that the transcriptional co-activator TAZ is expressed by the same cells that express αSMA in the epithelial compartment of the differentiating murine salivary gland and by mSG-PAC1 cells under conditions that promote a myoepithelial phenotype. Furthermore, siRNA targeting TAZ expression in mSG-PAC1 spheroids diminishes expression of myoepithelial markers, implicating TAZ in their regulation. Thus, we have demonstrated mSG-PAC1 cells are a reliable tool to complement *in vivo* approaches to understand mechanisms that promote myoepithelial differentiation.

Introduction

In many exocrine glands, such as the mammary, lacrimal, and salivary glands, myoepithelial cells serve as contractile units, which in response to environmental cues aid in the transport of gland specific secretions, and their dysfunction negatively affects secretory function (Chitturi et al., 2015; Garcia-Posadas et al., 2020; Makarenkova and Dartt, 2015; Raymond et al., 2011; Redman, 1994). Myoepithelial cells also contribute to the development and maintenance of the overall structure of the individual glands (Adriance et al., 2005; Gudjonsson et al., 2005; Makarenkova and Dartt, 2015; Redman, 1994; Sirka et al., 2018). Additionally, they serve as barriers that prevent dissemination of interior luminal cells, by serving as an interface between the basement membrane and luminal epithelial cells (Adriance et al., 2005; Gudjonsson et al., 2005; Makarenkova and Dartt, 2015; Sirka et al., 2018). Recent data suggest that myoepithelial cells also play an important role as reserve stem cells in tissue repair both in exocrine glands and other branched organs (Lynch et al., 2018; Makarenkova and Dartt, 2015; Ninche et al., 2020; Tata et al., 2018). In spite of their important physiological functions, little is known regarding mechanisms that regulate their differentiation.

Tissue regeneration has become the focus of investigation in multiple contexts and in the salivary gland in particular. Permanent salivary gland damage is a consequence of radiation therapy for head and neck cancers. In many cases, irreversible damage is concentrated in the saliva-producing acinar cells and myoepithelial cells of the submandibular salivary gland (Grundmann et al., 2009; Hakim et al., 2002; Vissink et al., 2010). Thus, much current research employing murine models is aimed at understanding mechanisms to regenerate salivary gland tissue, including the replacement of acinar and myoepithelial cells following damage induced by radiation, obstruction or resection (May et al., 2018; Ninche et al., 2020; OKeefe et al., 2020; Weng et al., 2018).

We have taken a complementary cell culture approach, which facilitates the identification of signaling pathways that guide differentiation events. In our previous studies, we established the murine salivary gland epithelial cell line, mSG-PAC-1 that recapitulates aspects of acinar cell differentiation in culture (Thiemann et al., 2019). Since the myoepithelial layer in the developing submandibular salivary gland differentiates from the outer cuboidal layer of epithelial cells, adopting myoepithelial properties, including a flattened morphology and the expression of alpha-smooth muscle actin (αSMA) (Gervais et al., 2016), we asked whether we could promote myoepithelial differentiation of mSG-PAC-1 cells, and if so, whether these cells could be used to gain insight into the molecular mechanisms involved. By altering the culture conditions for three-dimensional spheroids cultured in a laminin-rich matrix (Matrigel), we report that the outer mSG-

PAC1 cells are capable of differentiating into a myoepithelial layer characterized by cells that express myoepithelial markers and that adopt stellate cellular morphologies and flattened nuclei. Gene expression analysis implicated the transcriptional co-activators, Yes-associated protein/Transcriptional co-activator with PDZ-binding motif (YAP/TAZ) as potential regulators of this process. We found TAZ protein expression was upregulated during myoepithelial differentiation both in our cell culture model and during salivary gland development. Using siRNA-directed depletion, we demonstrated that TAZ regulates aspects of myoepithelial differentiation of mSG-PAC1 cells in culture. Thus, our data suggest that TAZ is an important contributor to the regulation of myoepithelial gene expression in culture, and may also regulate myoepithelial differentiation in the submandibular salivary gland.

RESULTS

mSG-PAC1 cells differentiate towards a myoepithelial phenotype in three-dimensional culture

Our previous studies described the establishment of the pro-acinar cell line (mSG-PAC1) that recapitulated aspects of acinar differentiation in three-dimensional cultures in Matrigel. Using this cell line, we demonstrated that the replacement of EGF with FGF2 in a modified MCF10A medium promoted pro-acinar differentiation by increasing the expression of the water channel protein, aquaporin 5 (AQP5) and establishing a polarized outer suprabasal cuboidal layer of cells of spheroids formed in Matrigel (Thiemann et al., 2019). In the current study, we will refer to this FGF2-containing medium as Pro-A for pro-acinar (see Materials and Methods).

Because the myoepithelial layer differentiates from the polarized outer cuboidal later of epithelial cells in developing salivary gland acini *in vivo* (Gervais et al., 2016), we sought to explore whether mSG-PAC1 cells could differentiate into myoepithelial cells. Others reported that the addition of serum to luminal epithelial cells from the mammary gland can contribute to their differentiation towards a myoepithelial phenotype (Pechoux et al., 1999). To test whether mSG-PAC1 cells could serve as progenitors cells of the myoepithelial phenotype, we compared the phenotype of spheroids cultured for six days in Matrigel with Pro-A medium described above or with Pro-M medium for pro-myoepithelial which consists of DMEM/F12 medium supplemented with 10% FBS (See Materials and Methods for details). Myoepithelial cells are characterized by their stellate shape with extended processes, flattened nuclear morphology, and expression of smooth muscle proteins important for contraction (Adriance et al., 2005). While mSG-PAC1 spheroids cultured in Pro-A medium maintained an organized structure with outer columnar cells at the basal edge, the cells at the basal edge of spheroids cultured in Pro-M medium adopted morphologies characteristic of myoepithelial cells and expressed the myoepithelial markers, alpha smooth muscle action (αSMA/*Acta2*) and calponin-1 (*Cnn1*) (Fig. 1A). Additionally, these spheroids displayed enhanced RNA expression of the integrin β4 subunit, which is also a myoepithelial marker (Gudjonsson et al., 2005) (Fig. 1B-C). Additionally, cells along the basal surface of spheroids cultured in Pro-M medium have significantly flatter nuclei compared to those cultured in Pro-A medium, quantitated by the increased ratio of nuclear diameter to height (Fig. 1E-F), which is characteristic of myoepithelial cells. Altogether, these data suggest that mSG-PAC1 cells are capable of differentiating from a pro-acinar to a myoepithelial-like phenotype in 3D culture, and that we have identified culture conditions that promote this process *in vitro*.

Transcriptome analysis reveals the Hippo signaling pathway as a potential regulator of myoepithelial differentiation

To gain insight into a possible mechanism involved in promoting the myoepithelial phenotype, we employed Clarion S microarrays to compare the transcriptome profiles of mSG-PAC1 cells cultured as spheroids in Matrigel for six days in Pro-M compared to Pro-A medium. We found that the expression of 3870 genes were changed by 2-fold or greater. The expression of 2183 genes were upregulated and 1678 were downregulated in Pro-M compared to Pro-A. The top five hundred genes upregulated in myoepithelial spheroids analyzed by the Transcriptome Analysis Console (TAC) (ThermoFisher) were compared to hallmark and curated gene sets available from the Molecular Signatures Database (MSigDB) available from the Broad Institute. Compared to spheroids cultured in Pro-A medium, spheroids cultured in Pro-M medium display enhanced gene expression in processes associated with tissue morphogenesis (Fig. 2A), cell differentiation (Fig. 2B), cell projection organization, cytoskeletal organization, and actin filament-based processes, among others (Fig. 2C). Not surprisingly, spheroids cultured Pro-M medium display significantly higher expression of myoepithelial genes, such as αSMA (*Acta2*) and calponin (*cnn2/cnn3*) (Fig. 3A). Moreover, these spheroids display a reduction in the expression of the acinar maturation marker, AQP5 (Fig. 3A), which phenocopies the reduction in expression observed by qPCR (Fig.1D). These data suggest that culturing mSG-PAC1 cells in Pro-M medium inhibits their acinar differentiation and promotes differentiation towards a myoepithelial lineage. Interestingly, several genes upregulated in Pro-M medium are established YAP/TAZ target genes, including many genes associated with canonical YAP/TAZ signaling, including connective tissue growth factor (*Ctgf*), cysteine-rich protein 61 (*Cyr61*), thrombospondin (*Thbs1*), Ajuba Lim protein (*Ajuba*), and ankyrin repeat domain 1 (*Ankrd1*) (Fig. 3B), suggesting YAP/TAZ signaling pathway may be important regulators of this differentiation event.

Subcellular localization of TAZ is associated with αSMA expression during morphogenesis of the SMG

Since many of the genes upregulated in the microarray were canonical target genes of YAP/TAZ, we sought to investigate their role in the differentiation of the myoepithelial layer in mSG-PAC1 cells. YAP/TAZ signaling has been reported to be important in the development and differentiation of branched organs (Enger et al., 2013; Mahoney et al., 2014; Skibinski et al., 2014; Szymaniak et al., 2017), and since TAZ has been implicated as a major regulator of

myoepithelial differentiation in the mammary gland (Skibinski et al., 2014), we asked whether TAZ contributed to myoepithelial differentiation in the murine submandibular salivary gland. We first compared the expression and subcellular localization of TAZ in the submandibular gland, at various stages of embryonic development (Fig. 4A). While TAZ was expressed at E14 and lasting through E19, its expression was increased in acini at E15 and E16 concurrent with the onset of myoepithelial differentiation (Gervais et al., 2016). Interestingly, there was also a switch in the subcellular localization of TAZ during this time. While TAZ seemed primarily cytosolic and junctional at E14 and E19, its localization appeared nuclear in a subset of suprabasal cells of developing acini at E15 and E16 (Fig. 4A). Moreover, this nuclear localization of TAZ was associated with αSMA expression in these cells, suggesting a possible relationship between TAZ activity and myoepithelial differentiation during salivary gland development (Fig.4B).

Myoepithelial spheroids display enhanced TAZ expression and signaling

To determine whether TAZ expression is altered when mSG-PAC1 spheroids are cultured for six days in Pro-M medium to promote a myoepithelial-like phenotype, we examined TAZ expression by immunofluorescence microscopy. The data revealed that TAZ expression was increased in spheroids cultured in Matrigel in Pro-M medium compared with those cultured in Pro-A medium (Fig. 5A), with a subset of cells displaying nuclear localization (Fig. 5A, insets). Moreover, these spheroids displayed enhanced expression of the canonical YAP/TAZ target genes, CTGF and CYR61 when compared to control spheroids (Fig. 5B-C), suggesting that TAZ expression and activity in epithelial cells contributes to the differentiation of the myoepithelial layer.

Inhibition of TAZ expression disrupts the expression of myoepithelial markers

Our data suggest that the expression and activity of TAZ contributes to the differentiation of the myoepithelial layer in mSG-PAC1 cells cultured in Matrigel. We next asked whether the expression of TAZ was required for the expression of myoepithelial markers. We treated Matrigel cultures of mSG-PAC1 cells in Pro-M medium with siRNA targeting TAZ. Two distinct siRNA sequences resulted in a significant reduction in TAZ expression levels (Fig. 5D and Fig. S1). Inhibiting TAZ expression did not significantly alter the expression of YAP or the acinar marker AQP5 (Fig. 5D and Fig. S1). However, there was a significant reduction in the expression of myoepithelial markers, αSMA and calponin using two independent siRNAs (Fig. 5D-E and Fig. S1), suggesting that TAZ plays an important role in the transcriptional regulation of these myoepithelial genes. Interestingly, the expression of the integrin β4 subunit was not

significantly altered by knockdown of TAZ, suggesting that the expression of the integrin β4 subunit is regulated by a different mechanism.

Comparison mSG-PAC1 transcriptome analysis with *in vivo* gene signatures

We next searched for patterns in the transcriptomes of mSG-PAC1 spheroids cultured in Pro-A or Pro-M-medium. Since a transcriptional profile for murine salivary gland myoepithelial cells, as well as acinar cells has recently become available (Hauser et al., 2020), we performed Gene-Set Enrichment Analyses (GSEA) using scRNA-seq data from this recent study. We found that genes expressed in salivary gland myoepithelial cells isolated from pups at postnatal day 1 (P1) and adult mice are most significantly enriched in mSG-PAC1 spheroids cultured in Pro-M medium as compared to spheroids cultured in Pro-A medium (Fig. 6A-B). Hauser and colleagues identified two proacinar clusters in the developing SMG based on their expression of submandibular gland protein C (Smgc) and parotid secretory protein (PSP/*Bpifa2*) (Hauser et al., 2020). Genes from both populations defined at P1, as well as those expressed by acinar cells in the adult are enriched in mSG-PAC1 spheroids cultured in Pro-A medium compared to Pro-M (Fig. 6C-E). Additionally, GSEA analysis using scRNA-seq data from the murine mammary gland showed that myoepithelial specific genes are modestly, but not significantly enriched in mSG-PAC1 spheroids cultured in Matrigel in Pro-M medium (Fig. S3A). This may be due to slight differences in gene expression in salivary gland and mammary gland myoepithelial cells. Interestingly, genes specific to luminal progenitor and mature luminal cells are significantly enriched mSG-PAC1 spheroids cultured in Matrigel in Pro-A medium (Fig. S3B-C). These data indicate that mSG-PAC1 cells show phenotypic plasticity, which can be influenced by culture conditions.

DISCUSSION

In our previous studies, we established a murine salivary gland epithelial cell line, mSG-PAC1, which recapitulates aspects of acinar differentiation when cultured in Matrigel using a modified MCF10A medium in which EGF is replaced with FGF2 (Thiemann et al., 2019), which we refer to here as Pro-A medium. In our current study, we demonstrate that the outer surface cells of mSG-PAC1 spheroids cultured in Matrigel in Pro-M medium differentiate into a myoepithelial-like layer, which is interesting as during the development of the murine salivary gland, myoepithelial cells differentiate from the outermost layer of epithelial cells of developing acini (Gervais et al., 2016). In Pro-M medium, mSG-PAC1 spheroids down regulate the acinar marker AQP5 and upregulate the expression of the myoepithelial markers α-SMA, calponin and the integrin β4 subunit. Additionally, the expression of the transcriptional co-activator TAZ is increased in mSG-PAC1 cells that assume a myoepithelial morphology and contributes to the regulation of α-SMA and calponin expression in these cells. Consistent with these findings, TAZ protein expression is also upregulated during SMG development at the onset of the expression of the myoepithelial marker, α-SMA.

Although we have identified conditions that promote the ability of mSG-PAC1 cells to recapitulate aspects of either acinar (Thiemann et al., 2019) or myoepithelial differentiation as reported here, we have not been able to identify culture conditions that allow mSG-PAC1 cells to differentiate into mature acinar or myoepithelial cells, or to simultaneously differentiate into both acinar and myoepithelial cells in the same Matrigel culture. Additional environmental signals, as well as medium components, are likely required to support their further differentiation. Notably, the addition of serum to Pro-A medium is not sufficient to promote mSG-PAC1 spheroids toward a myoepithelial phenotype. It is possible that some growth factors present in Pro-A medium have an inhibitory effect on myoepithelial differentiation. Indeed, FGF2 has been shown to inhibit YAP/TAZ-dependent transcription in some contexts (Eda et al., 2008). Thus, FGF2 may function to maintain a proacinar phenotype by suppressing YAP/TAZ activity in our system.

The downstream effectors of the Hippo signaling pathway, YAP/TAZ have been implicated as important regulators of development and differentiation in many branched organ systems, including the salivary gland (Enger et al., 2013; Kim et al., 2021; Mahoney et al., 2014; Skibinski et al., 2014; Szymaniak et al., 2017). In the developing murine salivary gland, mechanical cues regulate YAP/TAZ activity (Kim et al., 2021). Others have shown that YAP activation contributes to the expansion of ductal progenitors and that YAP regulation by the LATS kinases, a

component of the Hippo pathway, is required for proper ductal morphogenesis (Szymaniak et al., 2017). The activity of TAZ in the developing salivary gland is also regulated by the LATS kinases and this regulation is needed for normal branching morphogenesis (Enger et al., 2013). During morphogenesis, TAZ is localized at cell-cell junctions by a mechanism dependent upon LATS kinases. RNAi-mediated depletion of LATS resulted in defects in morphogenesis and loss of association of TAZ at cell-cell junctions similar to the localization of TAZ in the salivary glands of NOD mice, a murine model employed to study Sjögren's Syndrome (Enger et al., 2013). In our studies, we also examined the subcellular localization TAZ in embryonic buds at E14-E19. When we examined the subcellular localization TAZ during salivary gland development, we also found that TAZ was localized at cell-cell junctions in the majority of cells in epithelial buds at E15 and E16. However, in a subset of cells at the basal surface that expressed αSMA, TAZ localized to the nucleus. This localization is consistent with a role for TAZ in regulation myoepithelial differentiation in the developing salivary gland, as previously shown for mammary epithelial cells (Mahoney et al., 2014).Others have demonstrated that the interaction of cells with the basement membrane regulates the activation of YAP/TAZ (Chang et al., 2015; De Rosa et al., 2019; Elbediwy et al., 2016; Hu et al., 2017; Zhang et al., 2017). Thus, the interaction of outer cuboidal epithelial cells with the maturing basement membrane of developing buds of the salivary gland may activate TAZ to promote myoepithelial differentiation together with additional environmental cues. It will be important to directly demonstrate a functional role for TAZ in regulating myoepithelial differentiation during the development of the salivary gland *in vivo* and to determine whether integrin-mediated adhesion plays a role in this regulation.

In summary, we demonstrate that our previously characterized salivary gland epithelial cell line, mSG-PAC1, is capable of further differentiating into a myoepithelial-like layer in 3D Matrigel culture. Moreover, we identify TAZ as a regulator of myoepithelial differentiation in culture by regulating the transcription of myoepithelial genes. The expression pattern of TAZ during the differentiation of myoepithelial cells of the developing salivary gland is consistent with a similar role for TAZ *in vivo*.

Materials and methods

Cell Culture.

The establishment and characterization of the murine proacinar cell line, mSG-PAC1 was previously described (Thiemann et al., 2019). These cells were maintained in a modification of the culture medium previously described for the isolation of the mammary epithelial cell line MCF10A (Debnath et al., 2003; Soule et al., 1990), which consisted of DMEM/F12 supplemented with 5% donor horse serum (Atlanta Biologicals, #S12150), 100 U/ml penicillin/streptomycin (Hyclone, #SV30010), 20 ng/ml human recombinant EGF (Gibco, #PHG0311L), 100 ng/ml Cholera Toxin (Sigma, #C8052), 2.5 µg/ml hydrocortisone (Sigma, #H0396), and 20 µg/ml human insulin (Sigma, #I9278). To induce a more pro-acinar phenotype, human recombinant EGF was replaced with 100 ng/ml bFGF/FGF2 (Peprotech, #450-33) (Hosseini et al., 2018). This medium is referred to as Pro-A. To induce more myoepithelial characteristics, cells were cultured Pro-M medium, which consisted of DMEM/F12 medium supplemented with 10% FBS (Atlanta Biologicals, #S11150) and 100 U/ml penicillin/streptomycin (Hyclone, #SV30010). For three- dimensional (3D) spheroid cultures, matrices were prepared in 8-well chamber slides (Corning, #08-774-208). Matrices consisted of 100% Matrigel (Corning, #354230, protein concentration ~10 mg/ml, endotoxin <1.5 mg/ml). Approximately, 1000 cells were plated per well and cultured for 5-7 days in medium supplemented with 2% Matrigel in either Pro-A ore Pro-M medium as indicated in the Figure Legends.

Submandibular salivary gland explants

Murine submandibular salivary glands were dissected as previously described (Sequeira et al., 2013) from embryos harvested from timed-pregnant female mice (CD-1 strain, Charles River Laboratories) at E14, E15, E16, and E19 with E0 as designated by the discovery of a vaginal plug. Embryonic salivary glands were placed on Whatman® Nuclepore filters in 35 mm MatTek dishes (MatTek, #P35G-1.5-14-C) and fixed in 4% paraformaldehyde at 4°C overnight and then processed for immunostaining.

Immunostaining

Spheroids cultured in Matrigel were fixed for 20 min in 4% paraformaldehyde, washed in 0.5% PBST, permeabilized in 0.4% Triton-X-100/PBS for 20 min, and then washed in 0.5% PBST

before blocking 1-2 h in 20% donkey serum/PBST. Primary and secondary antibodies were incubated overnight in 3% BSA/PBST.

Submandibular glands were washed in 0.5% PBST after overnight fixation in 4% paraformaldehyde, permeabilized in 0.4% Triton-X-100/PBS for 30 min and then washed in 0.5% PBST before blocking 1-2 h in 20% donkey serum/PBST. Primary and secondary antibodies were incubated overnight in 3% BSA/PBST. All antibodies and dilutions used for immunofluorescence are listed in Table S2. DRAQ5 (Cell Signaling) was used at a dilution of 1:1000 to detect nuclei. Coverslips and slides were mounted using SlowFade®Gold antifade mounting medium (Life Technologies, #P36930).

RNA isolation & quantitative PCR (qPCR)

RNA was extracted with TRIzol (Ambion, ##15596026) and genomic DNA was removed with TURBO DNaseI (ThermoFisher Scientific, #AM1907) according to the manufacturers' protocols. cDNA was synthesized from 500 ng-1µg of RNA using the iScript Reverse Transcription Supermix kit (Biorad, #1708840). Equal concentrations of cDNA were used in the qPCR reactions with iQ or iTaq SYBR Green Supermix (Biorad, #170-8880; #1725120). Reactions were run in triplicate using the BioRad CFX96 Real-time C1000 Touch Thermal Cycler. Ct values were normalized to β-actin. A list of primer sequences can be found in Table S2

RNA interference

mSG-PAC1 cells were cultured in Matrigel in Pro-M medium for two days. After two days, the resulting spheroids were transfected with siRNA in OptiMEM over the course of two consecutive days using Lipofectamine RNAiMAX, according to the manufacturer's protocol. Non-targeting siRNA or siRNA targeting YAP or TAZ was transfected at a final concentration of 400 nM. Transfection medium was replaced with Pro-M medium and 2% Matrigel for 24 hours prior to processing for RNA. siRNA sequences can be found in Table S3.

RNA microarray and bioinformatic analysis

Microarrays were performed using RNA isolated as described above from mSG-PAC1 spheroids cultured in Matrigel in either Pro-A or Pro-M medium from three independent experiments. Samples were analyzed using the mouse Clariom® S array (Invitrogen, #902930) at the Center for Functional Genomics at The University at Albany Health Sciences Campus, Rensselaer, NY, and analyzed using the Transcriptome Analysis Console (TAC) 4.0 software from ThermoFisher. Principal component analysis (PCA) and volcano plots indicate that these

culture conditions promote significant differences in gene expression (Fig. S2A-B). Gene overlaps were computed using hallmark and curated gene sets from Molecular Signatures Database available from the Broad institute. Gene-set enrichment analysis was performed using GSEA software (Subramanian et al., 2005) from the Broad Institute with published scRNA-seq gene sets (Han et al., 2018; Hauser et al., 2020). Gene sets for myoepithelial, proacinar and acinar cells isolated from the murine submandibular salivary gland were downloaded from Supplementary Fig. 6 (Hauser et al., 2020). ScRNA-seq data sets from murine mammary glands for myoepithelial cells and luminal cells from pregnant females and luminal progenitor cells from virgin females were downloaded from Supplemental Table 5 (Han et al., 2018). In instances where gene sets were larger than recommended for use in GSEA, subsets of genes with the highest adjusted p values were generated for the analysis.

Microscopy

Images were acquired using an inverted Nikon TE2000-E microscope with phase contrast and epifluorescence, a Prior ProScanII motorized stage, and Nikon C1 confocal system with EZC1 and NIS-Elements acquisition software, or using the Zeiss LSM 880 confocal microscope with AiryScan on an AxioObserver.Z1 motorized inverted microscope with Zeiss ZEN2.3 software. Confocal images were acquired either at 40X, 63X, or 100X, and are represented as maximum projection images or single slices, as indicated in the figure legends. Images were processed and analyzed using the Imaris 9 software, where indicated in the Figure Legends.

Animal experiments

All animal experiments and procedures were performed in accordance with the Albany Medical College Institutional Animal Care and Use Committee (IACUC) regulations. In accordance with protocols approved by the Albany Medical College IACUC, mouse submandibular salivary glands (SMGs) were dissected from timed-pregnant female mice (strain CD-1, Charles River Laboratories) at embryonic day 14 (E14), 15(E15), 16 (E16) or 19 (E19) with the day of plug discovery designated as E0.

Statistical Analysis

Statistical analyses were performed using the GraphPad Prism software employing Student's T-tests as indicated in the Figure Legends. P values of <0.05 were deemed statistically significant.

Acknowledgements

The authors thank the Imaging Core of Albany Medical College for assistance in the preparation of immunofluorescence images and Debbie Moran for secretarial assistance.

Competing interests

The authors declare no competing or financial interests.

Funding

This research was supported by National Institutes of Health [R01-GM-51540 to S.E.L. and R01-DE-027953 to ML].

Data Availablity

Datasets will be made publicly available at the time of publication.

Author Contributions

Conceptualization: R.F.T., S.V.,J.L., M.L. and S.E.L; Methodology: R.F.T., S.V., N.M., J.L, M.L., S.E.L.; Formal analysis: R.F.T., S.V., N.M.; Investigation: R.F.T., S.V., M.S.; Resources: S.E.L. and M.L.; Data curation: S.E.L. Writing – original draft: R.F.T.; Writing -review & editing R.F.T., S.V., N.M., J. L., M.L., S.E.L.; Supervision: S.E.L., M.L., V.S.; Project Administration: S.E.L.; Funding acquisition: S.E.L., M.L.

References

Adriance, M.C., J.L. Inman, O.W. Petersen, and M.J. Bissell. 2005. Myoepithelial cells: good fences make good neighbors. *Breast Cancer Res*. 7:190-197.

Chang, C., H.L. Goel, H. Gao, B. Pursell, L.D. Shultz, D.L. Greiner, S. Ingerpuu, M. Patarroyo, S. Cao, E. Lim, J. Mao, K.K. McKee, P.D. Yurchenco, and A.M. Mercurio. 2015. A laminin 511 matrix is regulated by TAZ and functions as the ligand for the alpha6Bbeta1 integrin to sustain breast cancer stem cells. *Genes Dev*. 29:1-6.

Chitturi, R.T., V. Veeravarmal, R.M. Nirmal, and B.V. Reddy. 2015. Myoepithelial Cells (MEC) of the Salivary Glands in Health and Tumours. *J Clin Diagn Res*. 9:ZE14-18.

De Rosa, L., A. Secone Seconetti, G. De Santis, G. Pellacani, T. Hirsch, T. Rothoeft, N. Teig, G. Pellegrini, J.W. Bauer, and M. De Luca. 2019. Laminin 332-Dependent YAP Dysregulation Depletes Epidermal Stem Cells in Junctional Epidermolysis Bullosa. *Cell Rep*. 27:2036-2049 e2036.

Debnath, J., S.K. Muthuswamy, and J.S. Brugge. 2003. Morphogenesis and oncogenesis of MCF-10A mammary epithelial acini grown in three-dimensional basement membrane cultures. *Methods*. 30:256-268.

Eda, H., K. Aoki, K. Marumo, K. Fujii, and K. Ohkawa. 2008. FGF-2 signaling induces downregulation of TAZ protein in osteoblastic MC3T3-E1 cells. *Biochem Biophys Res Commun*. 366:471-475.

Elbediwy, A., Z.I. Vincent-Mistiaen, and B.J. Thompson. 2016. YAP and TAZ in epithelial stem cells: A sensor for cell polarity, mechanical forces and tissue damage. *Bioessays*. 38:644-653.

Enger, T.B., A. Samad-Zadeh, M.P. Bouchie, K. Skarstein, H.K. Galtung, T. Mera, J. Walker, A.S. Menko, X. Varelas, D.L. Faustman, J.L. Jensen, and M.A. Kukuruzinska. 2013. The Hippo signaling pathway is required for salivary gland development and its dysregulation is associated with Sjogren's syndrome. *Lab Invest*. 93:1203-1218.

Garcia-Posadas, L., R.R. Hodges, T.P. Utheim, O.K. Olstad, V. Delcroix, H.P. Makarenkova, and D.A. Dartt. 2020. Lacrimal Gland Myoepithelial Cells Are Altered in a Mouse Model of Dry Eye Disease. *Am J Pathol*. 190:2067-2079.

Gervais, E.M., S.J. Sequeira, W. Wang, S. Abraham, J.H. Kim, D. Leonard, K.A. DeSantis, and M. Larsen. 2016. Par-1b is required for morphogenesis and differentiation of myoepithelial cells during salivary gland development. *Organogenesis*. 12:194-216.

Grundmann, O., G.C. Mitchell, and K.H. Limesand. 2009. Sensitivity of salivary glands to radiation: from animal models to therapies. *J Dent Res*. 88:894-903.

Gudjonsson, T., M.C. Adriance, M.D. Sternlicht, O.W. Petersen, and M.J. Bissell. 2005. Myoepithelial cells: their origin and function in breast morphogenesis and neoplasia. *J Mammary Gland Biol Neoplasia*. 10:261-272.

Hakim, S.G., H. Kosmehl, I. Lauer, R. Nadrowitz, T. Wedel, and P. Sieg. 2002. The role of myoepithelial cells in the short-term radiogenic impairment of salivary glands. An immunohistochemical, ultrastructural and scintigraphic study. *Anticancer Res*. 22:4121-4128.

Han, X., R. Wang, Y. Zhou, L. Fei, H. Sun, S. Lai, A. Saadatpour, Z. Zhou, H. Chen, F. Ye, D. Huang, Y. Xu, W. Huang, M. Jiang, X. Jiang, J. Mao, Y. Chen, C. Lu, J. Xie, Q. Fang, Y. Wang, R. Yue, T. Li, H. Huang, S.H. Orkin, G.C. Yuan, M. Chen, and G. Guo. 2018. Mapping the Mouse Cell Atlas by Microwell-Seq. *Cell*. 172:1091-1107 e1017.

Hauser, B.R., M.H. Aure, M.C. Kelly, Genomics, C. Computational Biology, M.P. Hoffman, and A.M. Chibly. 2020. Generation of a Single-Cell RNAseq Atlas of Murine Salivary Gland Development. *iScience*. 23:101838.

Hosseini, Z.F., D.A. Nelson, N. Moskwa, L.M. Sfakis, J. Castracane, and M. Larsen. 2018. FGF2-dependent mesenchyme and laminin-111 are niche factors in salivary gland organoids. *J Cell Sci*. 131.

Hu, J.K., W. Du, S.J. Shelton, M.C. Oldham, C.M. DiPersio, and O.D. Klein. 2017. An FAK-YAP-mTOR Signaling Axis Regulates Stem Cell-Based Tissue Renewal in Mice. *Cell Stem Cell*. 21:91-106 e106.

Kim, J.M., Y. Jo, J.W. Jung, and K. Park. 2021. A mechanogenetic role for the actomyosin complex in branching morphogenesis of epithelial organs. *Development*. 148.

Lynch, T.J., P.J. Anderson, P.G. Rotti, S.R. Tyler, A.K. Crooke, S.H. Choi, D.T. Montoro, C.L. Silverman, W. Shahin, R. Zhao, C.W. Jensen-Cody, A. Adamcakova-Dodd, T.I.A. Evans, W. Xie, Y. Zhang, H. Mou, B.P. Herring, P.S. Thorne, J. Rajagopal, C. Yeaman, K.R. Parekh, and J.F. Engelhardt. 2018. Submucosal Gland Myoepithelial Cells Are Reserve Stem Cells That Can Regenerate Mouse Tracheal Epithelium. *Cell Stem Cell*. 22:779.

Mahoney, J.E., M. Mori, A.D. Szymaniak, X. Varelas, and W.V. Cardoso. 2014. The hippo pathway effector Yap controls patterning and differentiation of airway epithelial progenitors. *Dev Cell*. 30:137-150.

Makarenkova, H.P., and D.A. Dartt. 2015. Myoepithelial Cells: Their Origin and Function in Lacrimal Gland Morphogenesis, Homeostasis, and Repair. *Curr Mol Biol Rep*. 1:115-123.

May, A.J., N. Cruz-Pacheco, E. Emmerson, E.A. Gaylord, K. Seidel, S. Nathan, M.O. Muench, O.D. Klein, and S.M. Knox. 2018. Diverse progenitor cells preserve salivary gland ductal architecture after radiation-induced damage. *Development*. 145.

Ninche, N., M. Kwak, and S. Ghazizadeh. 2020. Diverse epithelial cell populations contribute to the regeneration of secretory units in injured salivary glands. *Development*. 147.

OKeefe, K.J., K.A. DeSantis, A.L. Altrieth, D.A. Nelson, E.Z.M. Taroc, A.R. Stabell, M.T. Pham, and M. Larsen. 2020. Regional Differences following Partial Salivary Gland Resection. *J Dent Res*. 99:79-88.

Pechoux, C., T. Gudjonsson, L. Ronnov-Jessen, M.J. Bissell, and O.W. Petersen. 1999. Human mammary luminal epithelial cells contain progenitors to myoepithelial cells. *Dev Biol*. 206:88-99.

Raymond, K., S. Cagnet, M. Kreft, H. Janssen, A. Sonnenberg, and M.A. Glukhova. 2011. Control of mammary myoepithelial cell contractile function by alpha3beta1 integrin signalling. *EMBO J*. 30:1896-1906.

Redman, R.S. 1994. Myoepithelium of salivary glands. *Microsc Res Tech*. 27:25-45.

Sequeira, S.J., E.M. Gervais, S. Ray, and M. Larsen. 2013. Genetic modification and recombination of salivary gland organ cultures. *J Vis Exp*:e50060.

Sirka, O.K., E.R. Shamir, and A.J. Ewald. 2018. Myoepithelial cells are a dynamic barrier to epithelial dissemination. *J Cell Biol*. 217:3368-3381.

Skibinski, A., J.L. Breindel, A. Prat, P. Galvan, E. Smith, A. Rolfs, P.B. Gupta, J. LaBaer, and C. Kuperwasser. 2014. The Hippo transducer TAZ interacts with the SWI/SNF complex to regulate breast epithelial lineage commitment. *Cell Rep*. 6:1059-1072.

Soule, H.D., T.M. Maloney, S.R. Wolman, W.D. Peterson, Jr., R. Brenz, C.M. McGrath, J. Russo, R.J. Pauley, R.F. Jones, and S.C. Brooks. 1990. Isolation and characterization of a spontaneously immortalized human breast epithelial cell line, MCF-10. *Cancer Res*. 50:6075-6086.

Subramanian, A., P. Tamayo, V.K. Mootha, S. Mukherjee, B.L. Ebert, M.A. Gillette, A. Paulovich, S.L. Pomeroy, T.R. Golub, E.S. Lander, and J.P. Mesirov. 2005. Gene set enrichment analysis: a knowledge-based approach for interpreting genome-wide expression profiles. *Proc Natl Acad Sci U S A*. 102:15545-15550.

Szymaniak, A.D., R. Mi, S.E. McCarthy, A.C. Gower, T.L. Reynolds, M. Mingueneau, M. Kukuruzinska, and X. Varelas. 2017. The Hippo pathway effector YAP is an essential regulator of ductal progenitor patterning in the mouse submandibular gland. *Elife*. 6.

Tata, A., Y. Kobayashi, R.D. Chow, J. Tran, A. Desai, A.J. Massri, T.J. McCord, M.D. Gunn, and P.R. Tata. 2018. Myoepithelial Cells of Submucosal Glands Can Function as Reserve Stem Cells to Regenerate Airways after Injury. *Cell Stem Cell*. 22:668-683 e666.

Thiemann, R.F., D.A. Nelson, C. Michael DiPersio, M. Larsen, and S.E. LaFlamme. 2019. Establishment of a Murine Pro-acinar Cell Line to Characterize Roles for FGF2 and alpha3beta1 Integrins in Regulating Pro-acinar Characteristics. *Sci Rep*. 9:10984.

Vissink, A., J.B. Mitchell, B.J. Baum, K.H. Limesand, S.B. Jensen, P.C. Fox, L.S. Elting, J.A. Langendijk, R.P. Coppes, and M.E. Reyland. 2010. Clinical management of salivary gland hypofunction and xerostomia in head-and-neck cancer patients: successes and barriers. *Int J Radiat Oncol Biol Phys*. 78:983-991.

Weng, P.L., M.H. Aure, T. Maruyama, and C.E. Ovitt. 2018. Limited Regeneration of Adult Salivary Glands after Severe Injury Involves Cellular Plasticity. *Cell Rep*. 24:1464-1470 e1463.

Zhang, D., S. Yang, E.M. Toledo, D. Gyllborg, C. Salto, J. Carlos Villaescusa, and E. Arenas. 2017. Niche-derived laminin-511 promotes midbrain dopaminergic neuron survival and differentiation through YAP. *Sci Signal*. 10.

Figure Legends

Figure 1. mSG-PAC1 cells can be induced to express myoepithelial markers and characteristics. (A) Representative confocal images of mSG-PAC1 spheroids cultured for six days in Matrigel in either a medium (Pro-A) that promoted pro-acinar phenotype or a medium (Pro-M) that promoted a myoepithelial phenotype and then immunostained for αSMA or calponin. Images are maximum projection images of five Z-slices acquired at 40X in 0.4 μm increments. Scale bar, 25 μm. Images are representative of three and two independent experiments for αSMA and calponin, respectively. **(B- D)** Relative mRNA expression of αSMA **(B)**, the integrin β4 subunit **(C)** or AQP5 **(D**) in mSG-PAC1 cells cultured for six days in Matrigel either in Pro-A or Pro-M medium. Expression is normalized to β-actin and then to expression in Pro-A condition. Data are from three independent experiments and plotted as the mean ± s.e.m. analyzed by Student's T-test. ND= not detected. **p<0.01, ****p<0.000. **(E-F)** mSG-PAC1 cells cultured in Pro-M medium display significantly flatter nuclei in cells at the basal periphery pf the spheroid. **(E)** Graphical representation of the method used to quantify nuclear shape using ImageJ. **(F)** Spheroids were cultured in either Pro-A or Pro-M medium for 6 days and immunostained for nuclei using DRAQ5. Width and height of nuclei relative to the basement membrane were quantitated in each cell at the basal periphery of spheroids using ImageJ Fiji. Data are from three independent experiments plotted as the mean nuclear width/height measured from eighteen spheres (n-18) ± s.e.m. analyzed by Student's T-test. ****p<0.0001.

Figure 2. Genes up regulated in mSG-PAC1 spheroids cultured in Pro-M medium. Gene microarrays were performed on RNA isolated from mSG-PAC1 spheroids cultured either in Pro-A or Pro-M medium. N=3 independent experiments. The top 500 genes most highly expressed by spheroids cultured in the Pro-M medium compared to those expressed in Pro-A M were used to compute overlap with hallmark and curated gene seta from Molecular Signatures Database (MSigDB) from the Broad institute. Genes more highly expressed in the Pro-M conditions are associated with **(A)** tissue, **(B)** cellular, and **(C)** myoepithelial developmental processes.

Figure 3. mSG-PAC1 spheroids cultured in Pro-M medium up regulate myoepithelial markers & YAP/TAZ target genes. (A) List of myoepithelial genes upregulated in mSG-PAC1 spheroids Pro-M medium cultured in for six days. Data is presented as the fold increase compared to spheroids cultured in Pro-A medium. **(B)** List of YAP/TAZ target genes upregulated

in by spheroids cultured Pro-M medium. Data is presented as the fold increase compared to spheroids cultured in Pro-A medium.

Figure 4. Expression of TAZ and αSMA during SMG morphogenesis. (A) Representative confocal images of embryonic SMGs (E14-E19) immunostained for TAZ and DNA. Images are a single Z-slice acquired at 63X representative of four SMGs. Insets represent a magnified view of TAZ and DNA around the basal edge of each proacinus. White arrows emphasize the co-localization of TAZ and the nuclear marker DRAQ5. White arrowheads emphasize nuclei showing no TAZ co-localization. Scale bar, 5 μm. **(B-C)** Expression of αSMA expression and TAZ in E15 and E16 SMGs. Representative confocal images of E15 (B) and E16 (C) SMGs immunostained for TAZ, αSMA, and DNA. White arrows represent cells with αSMA expression and with TAZ co-localization with the nuclear marker DRAQ5. White arrowhead indicates a representative cell lacking SMA expression and also the lack of TAZ co-localization with the nuclear marker DRAQ5. Images are single z-slices acquired at 63x. Size bar, 5 μm. (A-C) Images are representative of 4 SMGs per timepoint.

Figure 5. mSG-PAC1 cells cultured in Pro-M medium display characteristics of myoepithelial cells. (A) Increased expression of TAZ in the cells at the periphery mSG-PAC1 spheroids cultured in Pro-M. Representative confocal images from 2 independent experiments of mSG-PAC1 cells cultured for six days in Matrigel in either Pro-A or Pro-M medium and immunostained for TAZ (red) and DRAQ5 (pseudocolored blue). Insets represent a magnified view of nuclear staining. Images are maximum projection images of two z-slices acquired at 40X in 0.4 μm steps. Size bar, 25 μm. **(B,C)** Relative mRNA expression of YAP/TAZ target genes, CTGF **(B)** and CYR61 **(C)**, in mSG-PAC1 cells cultured in Matrigel in either Pro-A or Pro-M medium. Expression normalized to β-actin and the expression in Pro-A medium. Data are from three independent experiments plotted as the mean ± s.e.m. analyzed by Student's T-test. **p<0.01; ***p<0.001. **(D)** SiRNA targeting TAZ expression inhibits the expression of αSMA. Plotted is the relative mRNA expression of YAP, TAZ, AQP5, and αSMA in mSG-PAC1 spheroids cultured in Matrigel in Pro-M medium. Expression is normalized to β-actin and the expression in cells treated with non-targeting (NT) siRNA. Data are from 4 independent experiments and plotted as the mean ± s.e.m. analyzed by Student's T-test. *ns*, not significant, **p<0.01; ***p<0.001; ****p<0.0001. **(E)** SiRNA targeting TAZ also inhibited the expression of calponin, but not the expression of the integrin β4 subunit. Plotted is the relative RNA

expression of TAZ, calponin, and the integrin β4 subunit in mSG-PAC1 spheroids cultured in Matrigel and Pro-M medium. Expression is normalized to β-actin and the expression of these genes after treatment with NT siRNA. Data are from three (calponin) and four (TAZ, Integrin β4) independent experiments and plotted as the mean ± s.e.m. analyzed by Student's T-test. *ns*, not significant, **p<0.01.

Figure 6. The culture of mSG-PAC1 spheroids in Pro-M or Pro-A results in the expression of myoepithelial or acinar enriched genes respectively. GSEA using scRNA-seq gene-sets generated from murine SMG from P1 pups or adult mice (Hauser et al., 2020) showed murine myoepithelial gene upregulation in Pro-M medium and murine acinar gene upregulation in Pro-A medium. **(A-B)** myoepithelial cells from P1 and adult mice, **(C-D)** proacinar cells from the *Smgc* and PSP clusters from P1, and **(E)** acinar cells from adult mice. NES = Normalized Enrichment Score and FDR = False Discovery Rate. *FDR q-value < 0.25 represent significant enrichment.

Table S1: Antibody Dilutions & Applications

Antibody	Company	Catalog #	Dilution	Application
Primary Antibodies				
αSMA	Sigma Aldrich	A5228	1:1000	ICC
TAZ	Sigma Aldrich	T4077	1:200	ICC
Calponin	Abcam	Ab46794	1:600	ICC
Secondary Antibodies				
AF568 Donkey anti-Rabbit	Alexa-Fluor	A10042	1:1000 (2D) 1:500 (3D)	ICC
AF488 Donkey anti-Mouse	Alexa-Fluor	A21202	1:1000 (2D) 1:500 (3D)	ICC
DRAQ5	Cell Signaling Technology	4084	1:1000 (2D) 1:500 (3D)	ICC

Table II qPCR Primer Sequences

Gene Product	Strand	Sequence (5'-3')
αSMA	Forward	GTCCCAGACATCAGGGAGTAA
	Reverse	TCGGATACTTCAGCGTCAGGA
AQP5	Forward	AGAAGGAGGTGTGTTCAGTTGC
	Reverse	GCCAGAGTAATGGCCGGAT
Calponin	Forward	GCACATTTTAACCGAGGTCCT
	Reverse	CTGATGGTCGTATTTCTGGGC
CTGF	Forward	CTCCACCCGAGTTACCAATG
	Reverse	TGGCGATTTTAGGTGTCC
CYR61	Forward	ACCAATGACAACCCAGAGTG
	Reverse	AAGTAAATCTGACTGGTTCTGGG
Integrin α3 subunit	Forward	CCTCTTCGGCTACTCGGTC
	Reverse	CCGGTTGGTATAGTCATCACCC
Integrin α6 subunit	Forward	TGCAGAGGGCGAACAGAAC
	Reverse	GCACACGTCACCACTTTGC
Integrin β4 subunit	Forward	ACTCCATGTCTGACGATCTGG
	Reverse	GGGACGCTGACTTTGTCCAC
Laminin α1	Forward	ATTTAGCCAATGGAAAGTGG
	Reverse	TTTTCTTACAAAGACACGGC
Laminin α5	Forward	TGTTTTTGTACAGCGACTTC
	Reverse	CTACGCTTACATTGACACTC
TAZ	Forward	GTGTGCCCAATGCACTGA
	Reverse	TGACGCATCCTAATCCTCTCTC
β-actin	Forward	GGCTGTATTCCCCTCCATCG
	Reverse	CCAGTTGGTAACAATGCCATGT

Table III siRNA sequences

Gene Name	Catalog Number	Company	Sequence
WWTR1 (TAZ), Sequence 1	Custom	Dharmacon	CAGAAUGACUUUAGAGAAUUU
WWTR1 (TAZ), Sequence 2	J-041057-09- 0002	Dharmacon	CAAUUUAUGUCCACGUUAA

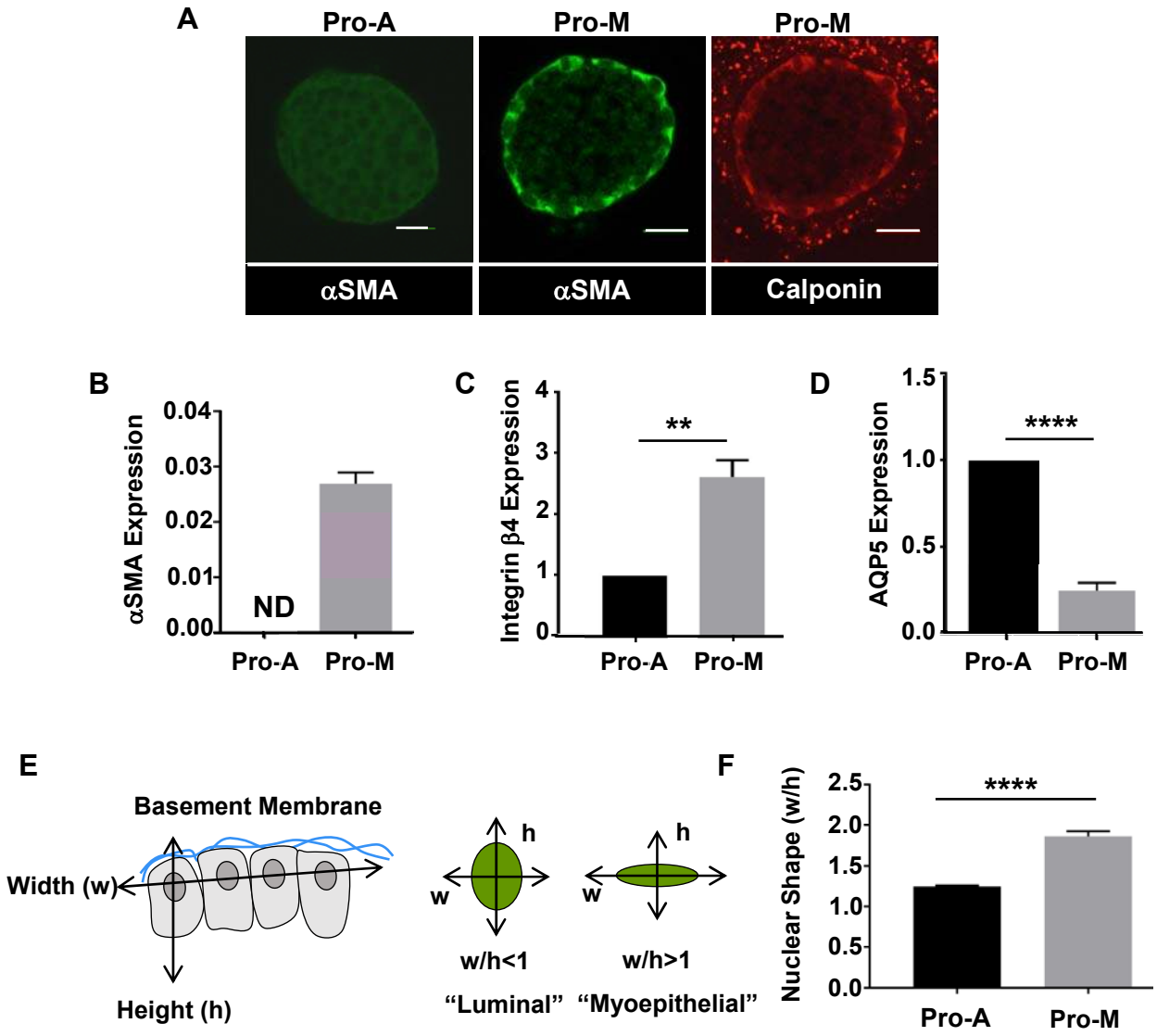

Figure 1

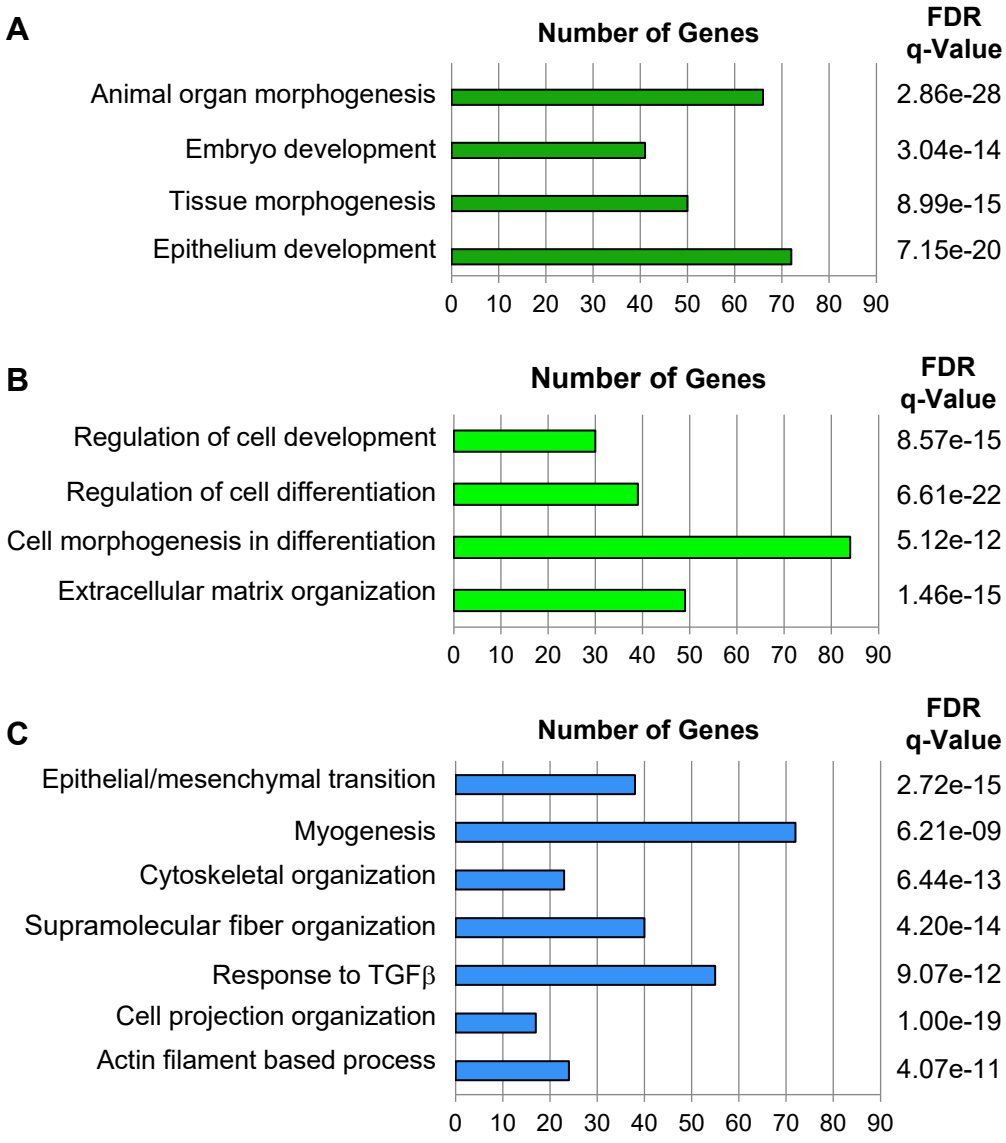

Figure 2

A

Gene	Common Name	Fold Change	P-value
Thbs1	Thrombospondin	5674.39	1.88e-06
Acta2	α-Smooth muscle actin	1325.38	1.92e-09
Mylip	Myosin regulatory light chain interacting protein	8.21	0.0003
Cald1	Caldesmon	5.64	0.0014
Cnn2	Calponin2	3.26	0.0158
Cnn3	Calponin3	2.86	0.0031
My110	Myosin light chain 10	1.42	0.0334
Myh10	Myosin heaving chain 10	1.33	0.0358
Aqp5	Aquaporin5	-5.99	0.0015

B

Gene	Common Name	Fold Change	P-value
Thbs1	Thrombospondin	5674.39	1.88e-06
Ajuba	Ajuba Lim protein	39.23	0.0003
Ctgf	Connective tissue growth factor	23.38	6.33e-06
Crim1	Cysteine-rich transmembrane BMP regulator 1	16.75	0.0011
Amotl2	Angiomotin-like 1	10.45	0.001
Tgfb2	Transforming growth factor, beta2	10.13	1.3e-06
Ankrd1	Ankyrin repeat domain 1	9.63	0.0005
Cyr61	Cysteine-rich protein 61	8.37	0.0002
Wwc2	WW,C2 and c oiled-coil domain containing 2	7.74	0.0003
Dlc1	Deleted in liver cancer 1	6.54	0.0003

Figure 3

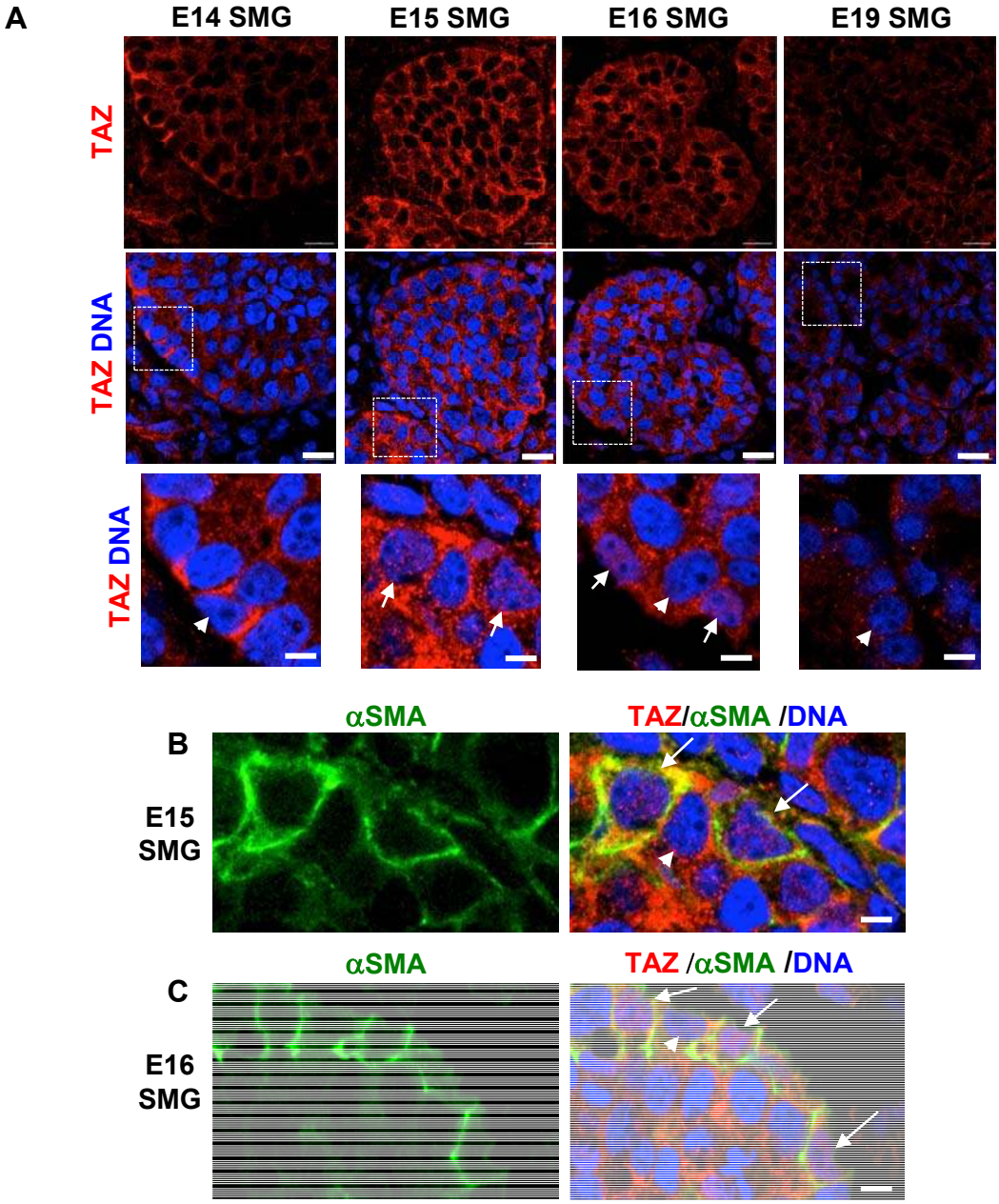

Figure 4

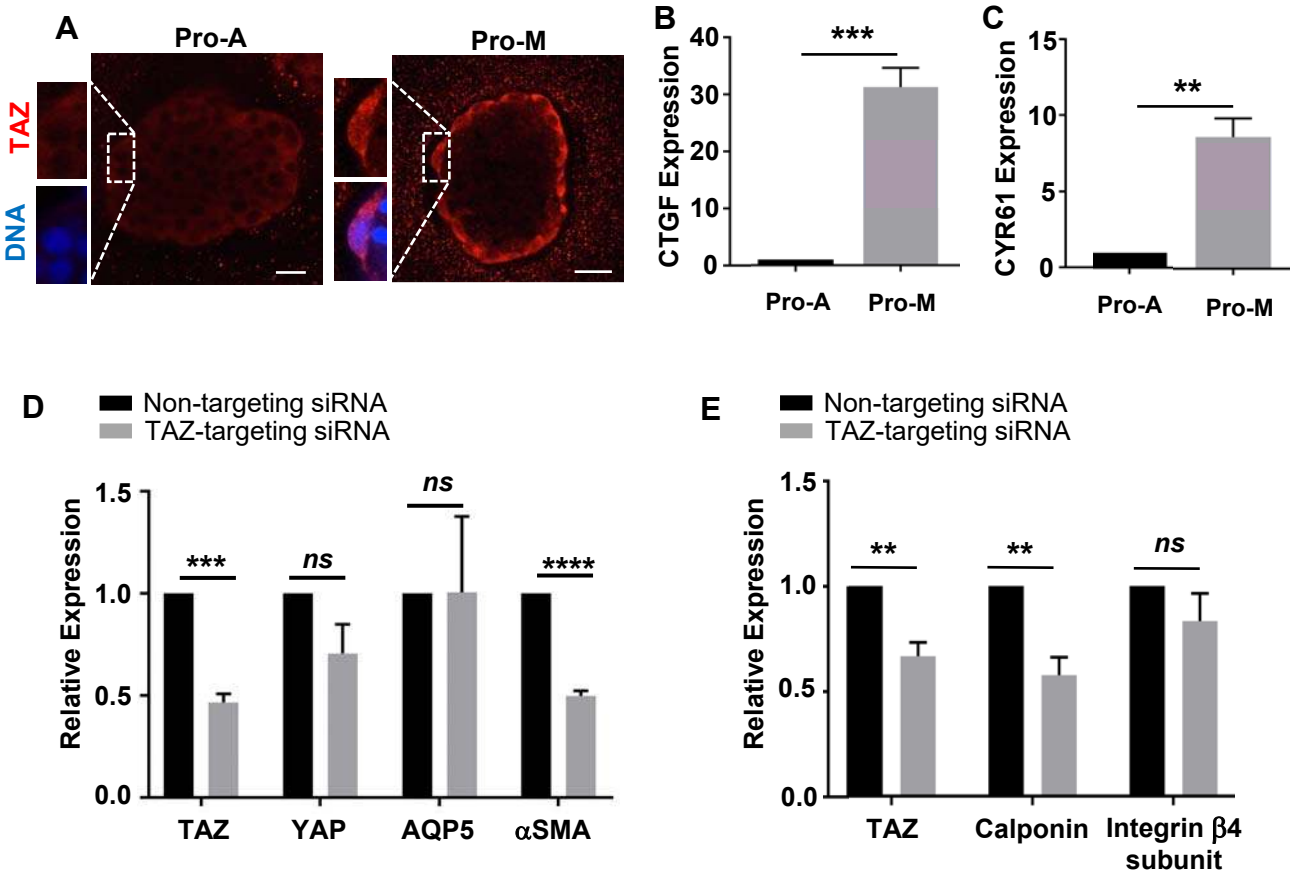

Figure 5

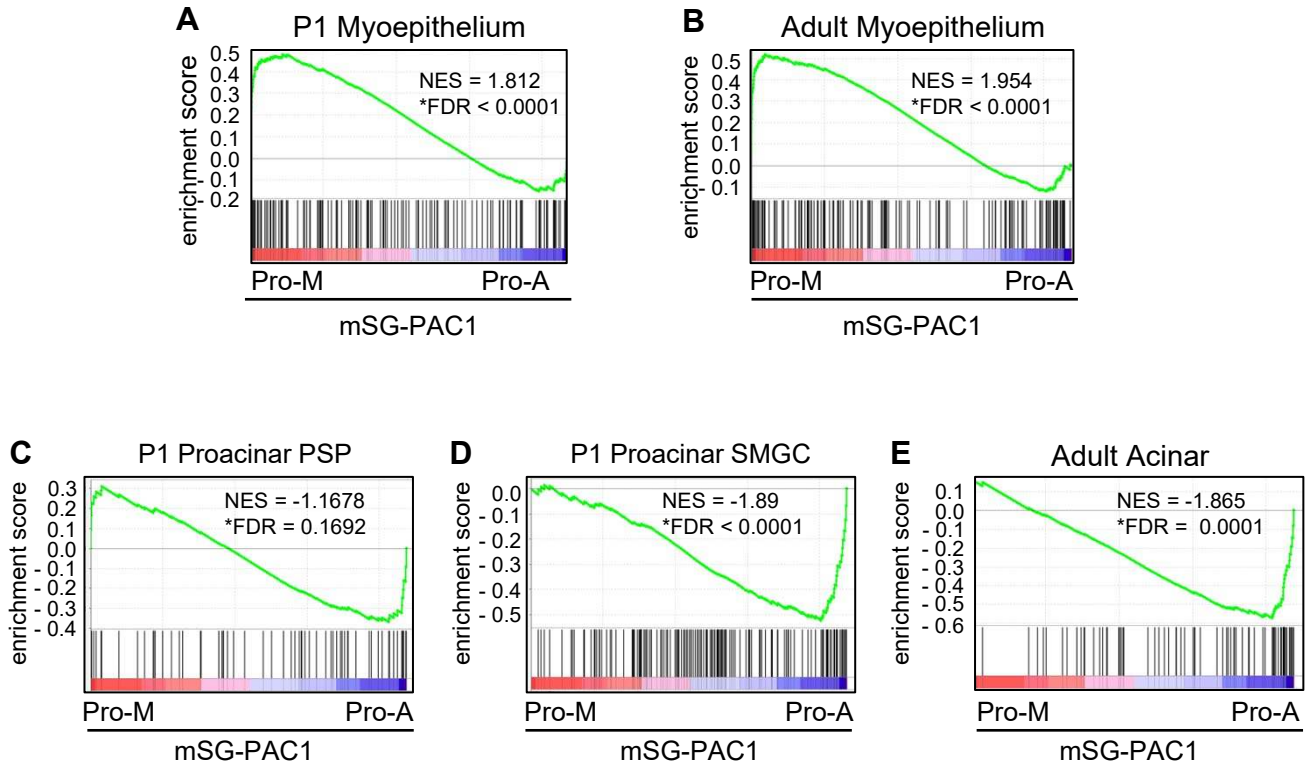

Figure 6

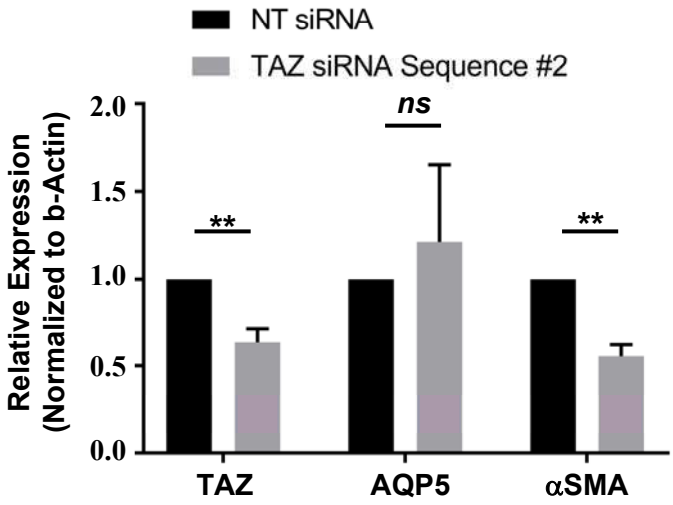

Supplementary Figure 1. TAZ depletion using a second siRNA sequence also inhibits the expression of αSMA without significantly affecting the expression of AQP5.

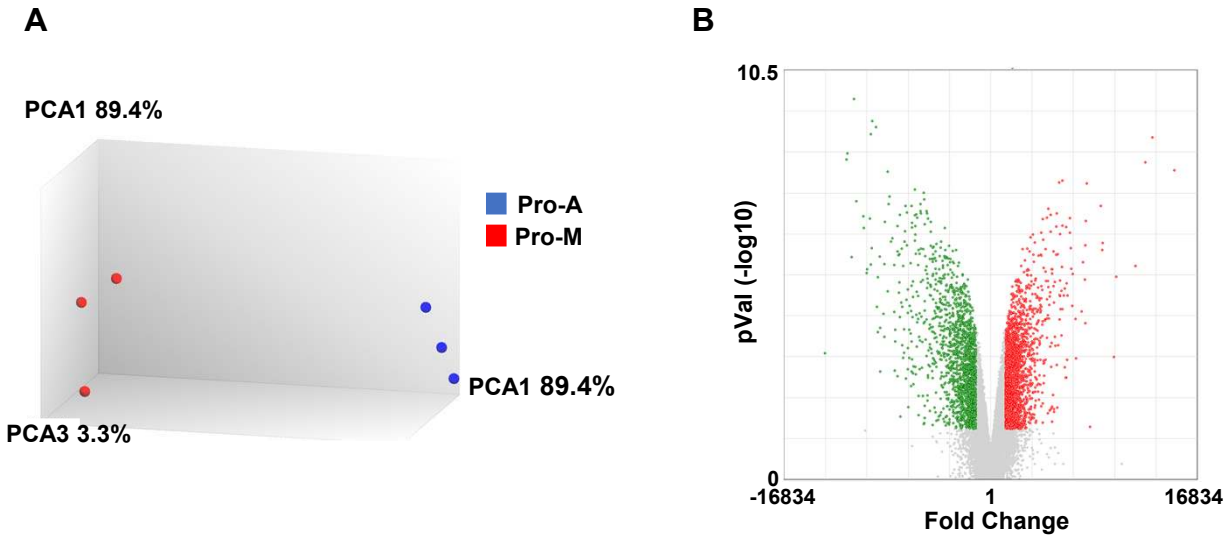

Supplementary Figure 2. (A) Principal component analysis (PCA) was performed to examine the variance between samples. **(B)** Volcano plot for differentially expressed genes in spheroids cultured in Pro-M compared to Pro-A medium. Genes increased by a factor of greater than 2-fold are shown in red and those that decreased by a factor of greater than 2-fold are shown in green.

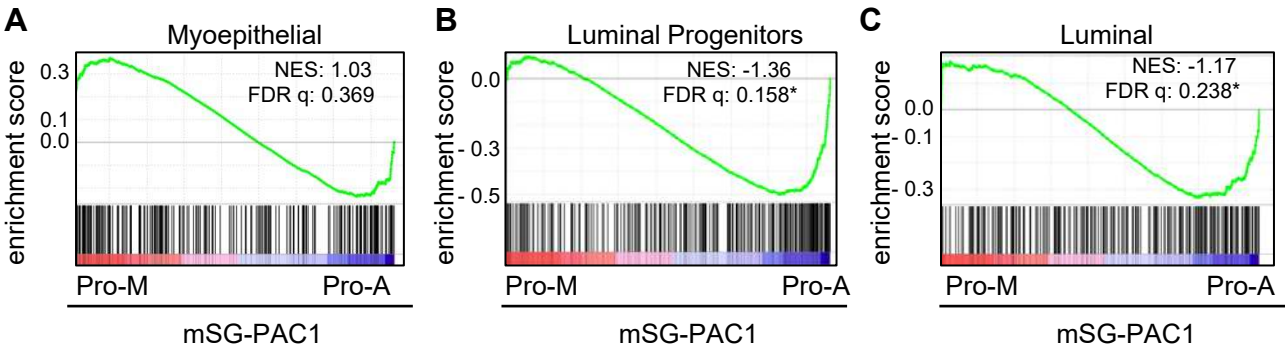

Supplementary Figure 3. Distinct differentiation programs are engaged in mSG-PAC1 spheroids cultured in Pro-A and Pro-M. GSEA was performed using gene sets derived from single cell RNA sequencing (scRNAseq) for myoepithelial cells and luminal cells from the mammary gland from pregnant females and luminal progenitor cells from virgin females. Data sets were downloaded from Supplemental Table 5 data for each cell type (Han et al., 2018). The analysis was performed using the 250 genes with the lowest adjusted p-value. **(A)** Myoepithelial specific genes are modestly, but not significantly enriched in mSG-PAC1 spheroids cultured in Matrigel in Pro-M medium (NES = 1.03, FDR q-value = 0.369). **(B)** Genes specific to luminal progenitor (NES = -1.36, FDR q-value = 0.158) and **(C)** mature luminal cells (NES= -1.17, FDR q-value = 0.238) are significantly enriched mSG-PAC1 spheroids cultured in Matrigel in Pro-A medium (FDR q-value < 0.25 represent significant enrichment.